

CHROMOSPHERIC FLARES AND 210 MHz RADIO EMISSION

M. Gigolashvili, N. Ograpishvili, D. Japaridze, Sh. Makandarashvili, B. Chargeishvili, and D. Maghradze

This is a study of the development of sixteen chromospheric flares observed at the Abastumani Astrophysical Observatory in 1973. $H\alpha$ filtergrams and radio bursts at a frequency of 210 MHz ($\lambda=1.43$ m) are examined. The $H\alpha$ filtergrams were obtained using a chromosphere-photosphere telescope with the aid of an interference polarization filter and the radio bursts were detected using the radio telescope at the Abastumani Observatory. The main purpose of this work is to detect radio signals associated with the flares. In most cases the area of the flare and its intensity reached their maxima almost simultaneously. As for the peak energy release, in most cases it reached a maximum at almost the same time or slightly earlier in the meter radio wavelength band than in the $H\alpha$ line. The sequence of events in the optical and radio bands during the flares is obtained by using the method of epoch superposition.

Keywords: chromospheric flares: $H\alpha$ filtergrams: radio bursts at 210 MHz

1. Introduction

A solar flare represents the reaction of the solar atmosphere to a sudden rapid release of energy that leads primarily to localized transient heating and acceleration of electrons, protons, and heavy ions. A flare generates short-duration electromagnetic emission over a wide range of wavelengths from hard x-rays ($\lambda \approx 10^{-9}$ cm) and, in very rare cases, gamma radiation ($\lambda \approx 2 \cdot 10^{-11}$ cm) to kilometer radio waves. Some chromospheric flares are accompanied by

E. K. Kharadze Abastumani Astrophysical Observatory, Ilia State University, Tbilisi, Georgia, e-mail: marina.gigolashvili@iliauni.edu.ge; natela.ograpishvili@iliauni.edu.ge; darejan.japaridze@iliauni.edu.ge; bidzina@aidio.net; davit.maghradze.2@iliauni.edu.ge

large bursts of radio emission.

Studies of the solar radio emission make a large contribution to our understanding of the physical processes taking place in the solar atmosphere and they make it possible to examine processes taking place in the solar corona.

The relationship of radio bursts and solar flares has been pointed out [1-3]. Dodson [4] and Dodson and Hedeman [5-6] discovered that flares coincide with or precede radio storms at 200 MHz (150 cm). These flares may have a complicated structure and some have been referred to as “multiple bursts.” The characteristic feature of the flares associated with radio bursts is a smoother rise to their maximum than for most other flares.

De Feiter, et al. [7], have pointed out that strong flares are usually accompanied by radio bursts at decimeter and/or meter wavelengths. Only an insignificant part of the less important flares produce distinctive radio signals [7]. A correlation has been obtained with the aid of identification of the recorded flares and the use of diagrams and spectrograms for these sources. Observations were made to detect radio blackout and to detect the features of a flare.

Swarup, et al. [8], found that 60% of the fast (type III) radio bursts are coincident in time with solar flares. The coupled bursts usually occur between the onset and the maximum of a flare. It was also found that 25% of all solar flares are obviously related to fast bursts. Almost all slow bursts (type II) and continuous phenomena (type IV) are also associated with flares, but there is no distinct relationship between radio storm bursts (type I) and flares.

Radio emission from solar flares will require many unique diagnostic instruments to explain the energy release, plasma heating, particle acceleration, and transport of particles in the magnetized plasma [9].

Based on radio, x-ray, and magnetic field measurements of solar active region in 1992 (including high resolution radio, x-ray, magnetographic and H α observations), Vourlidas, et al. [10] attributed the excess emission of o-modes to the magnetic field configuration and to temperature inhomogeneities in a spot.

Krucker, et al. [11], suggested that solar flares and SXR/radio phenomena have some common features.

Shibasaki, et al. [12], have suggested that solar radio emission provides valuable information about the structure and dynamics of the solar atmosphere above a temperature minimum. They have examined new observational and theoretical data on the quiet sun and active regions over the entire radio wavelength range from millimeters to dekameters. They tried to provide as complete as possible a picture of the quiet sun and active regions with the aid of the radio regions. In principle, the radio range can give us as much information as the rest of the spectrum of the solar atmosphere.

A comparison of the radio fluxes at 10.7 cm with the number of solar spots for solar cycles 19-21 has shown that the values of the radio flux are related to the magnetic field associated with sunspots. Data on the radio flux at 10.7 cm and its relationship to the number of sunspots and other parameters were given for each of these cycles. These data showed that the radio flux at 10.7 cm appears to be stochastic for cycle 19 and chaotic for cycles 20 and 21 [13].

A mathematical model has been developed for calculating the structure of the dynamic spectra of radio bursts [14]. A comparison of the theoretical and observed spectra shows that interference explains the formation of zebra structures and the separation of the stripes into separate peaks, describes the time profile of the peaks, and explain the properties of the filaments, filament loops, and network of burst “points.” The similarity of the dynamic spectra shows that the microstructure of the spectra is formed as the waves propagate in the solar corona and interplanetary medium, rather than in the emission source.

Long-term observations of solar radio bursts at the Abastumani Astrophysical Observatory with the 210 MHz solar radio telescope have yielded a clear correlation between the amplitudes of the radio bursts and the number of sunspots and sunspot regions [15].

Radio frequency measurements have the advantage of providing high resolution with respect to altitude in the corona; this is because of the clear dependence of the propagation velocity of radio waves on the density of a medium. The high altitudes from which ultrashort (meter) emission reaches us are indicative of the distance from the sun at which we can study the corona by means of radio techniques.

Radio astronomy and optical astronomy, therefore, essentially supplement one another. The relationship of the radio emission from radio bursts and the magnetic field of an active region and flares, as well as the structure of sources in the corona and their sizes, are still unsolved problems.

Answers to these problems would help us determine the mechanism for the emission, explain the polarization, and use radio emission as an indicator of the state of the local magnetic fields in the solar corona upon which various geophysical phenomena depend.

Radio observations of the sun have been made at Abastumani since 1957. Very rich data have been acquired over that time.

The radio telescope used to detect the solar radio emission consists of three main parts: the feeder system antennas, a radiometer with a chart recorder, and a power supply.

The receiver part of the radio telescope is tuned to 210 MHz ($\lambda = 1.43$ m). The recorder records the overall solar radio flux and detects different bursts, including noise storms.

Elevated background (continuum) emission with superimposed transient bursts lasting from fractions of a second to seconds is referred to as a solar noise storm in the meter radio range.

These observations are very important for studying of fundamental problems of solar-terrestrial links. In particular, they can be used for long-term weather prediction.

2. Observational data and method of measurement

In this paper we describe plots of the development of chromospheric flares observed at the Abastumani Astrophysical Observatory in 1973 using the chromosphere-photosphere telescope with an H α -line interference-polarization optical filter with a passband of 0.5 Å. H α images of the active region were recorded on Tip-17 plates. H α images were taken at a rate of about 2 frames per minute in a daily observation program (from sunrise to sunset).

We studied the varying area and intensity of the flares, and when the energy release approached a maximum at the radio frequency, in the H α line as well.

We have chosen 16 flares, mostly of scale $1n$. The data are listed in Table 1. The longitudes are given in the heliocentric (λ) and Carrington (L) systems. The power of the flares was estimated on a four point scale: f faint, 1 normal, 2 powerful, and 3 most powerful. In the comments A indicates an eruptive protuberance with a base at a heliocentric distance of at least 90°; B , an observed flare which is the conclusion of a stronger one; C , a flare that was

TABLE 1. Parameters of Flares

| No. | Date | Time of observations | | | Coordinates | | | Power | Com- ment |
|-----|-------|---------------------------------|---------------------------------|---------------------------------|-------------|-----------|-------|-------|--------------|
| | | onset | end | maximum | ϕ | λ | L_0 | | |
| 1 | 19.06 | 08 ^h 03 ^m | 08 ^h 36 ^m | 08 ^h 17 ^m | -02 | -83 | 044 | 1n | D |
| 2 | 06.07 | 07 28 | 07 45 | 07 32 | -08 | +14 | 280 | 1n | D |
| 3 | 07.07 | 05 16 | 05 41 | 05 17 | -06 | +25 | 278 | 1n | B |
| 4 | 07.07 | 06 09 | 06 43 | 06 13 | +12 | +23 | 276 | 1n | C |
| 5 | 09.07 | 05 02 | 06 50 | 05 15 | +11 | +49 | 272 | 1n | D |
| 6 | 10.07 | 07 00 | 07 09 | 07 04 | +12 | +64 | 277 | 1n | E |
| 7 | 31.08 | 07 51 | 08 05 | 07 58 | -17 | -51 | 191 | 1n | D |
| 8 | 02.09 | 05 35 | 06 35 | 05 41 | -17 | -56 | 160 | 1n | C |
| 9 | 11.09 | 06 55 | 07 20 | 07 01 | -12 | +58 | 155 | 2n | B |
| 10 | 11.09 | 07 58 | 08 27 | 08 04 | -12 | +41 | 138 | 1n | B |
| 11 | 27.09 | 11 07 | 11 38 | 11 11 | -16 | -48 | 195 | 2n | B |
| 12 | 29.09 | 04 07 | 05 06 | 04 50 | +16 | -57 | 163 | 2n | B |
| 13 | 26.11 | 07 04 | 07 13 | 07 06 | -08 | -15 | 160 | 1n | D |
| 14 | 16.12 | 05 35 | 06 20 | 05 50 | -18 | -88 | 182 | 1n | A |
| 15 | 23.12 | 07 51 | 08 15 | 07 58 | -16 | +36 | 214 | 1n | A |
| 16 | 24.12 | 10 36 | 10 59 | 10 46 | -16 | +51 | 214 | 1n | C |

not visible ten minutes earlier, when there were no observations prior to the onset of the flare; *D*, a bright point; and, *E*, two or more bright points (flaring simultaneously). ϕ is the latitude, λ is the longitude, and $L = L_0 + \lambda$ (with L_0 being the latitude of the central meridian of the sun).

Photometric measurements of the flares were made on an MF-2 microphotometer. If a chromospheric flare consisted of several centers, separate measurements were made for each center. We tried to measure the same geometric site on a given flare from the time of its onset to its termination. Nodes of a flare that showed up later were measured separately.

In the following figures, the abscissa is time, the left ordinate is the intensity of the flares relative to the unperturbed chromosphere, and the right ordinate is the area of the flares in millionths of the solar disk area. If a flare consisted of several centers, then the intensities are given for each. But the centers of flares are difficult to distinguish by area, so we show plots of the variation in the overall area for all the centers together. Each figure includes a photograph of the flare at the time of its maximum.

Flare No. 1. June 19, 1973. (8:03-8:36 UT).

In the eastern edge of the solar disk in the active region near the spot an activity center stood out at 8:03 UT,

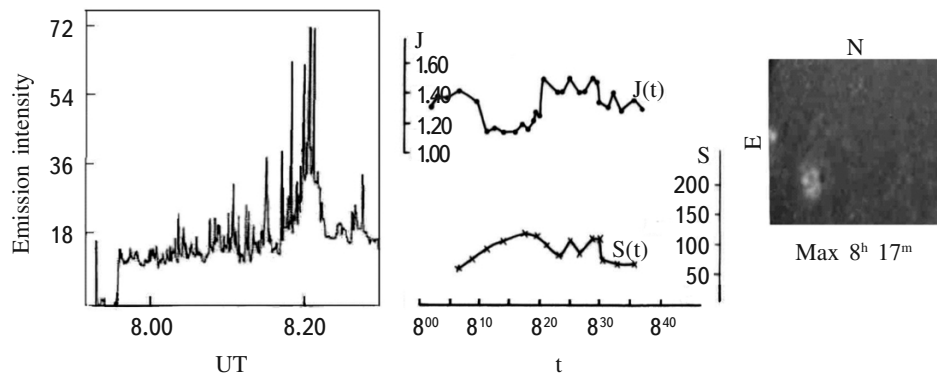


Fig. 1. Observations of flare No. 1. Left frame: variation in the radio frequency flux. Center frame: intensity and area of the flare. Right: observations in the $H\alpha$ line.

but even before 8:00 UT this part of the flocculus was fairly intense. Four minutes later a second, less bright active center appeared. Afterward, these centers merged and at 8:11-8:16 UT the intensity was observed to fall.

The flare reached a maximum intensity at 8:20 UT, and, in terms of area, still earlier at 8:15 UT. After the intensity maximum the flocculus and flare decreased. The flare has gone out at 8:36 UT, but an active site could be seen in the flocculus to the end of the observations (8:40 UT). Parallel observations were made in the radio range at 210 MHz ($\lambda = 1.43$ m). A radio burst with a high intensity of $I = 78 \cdot 10^{-22}$ W/m²/Hz could be seen at 8:20 UT. From 8:00-8:20 UT an elevated continuous noise level was observed with alternating individual bursts of high and low amplitudes $I = 18-36 \cdot 10^{-22}$ W/m²/Hz. These noise storms also continued after 8:20 UT. At this time we can say that the maximum energy release was almost simultaneous at the optical and meter wavelengths.

Flare No. 2. July 6, 1973. (7:28-7:32 UT).

In a large flocculus in the southwest solar disk two activity centers appeared almost simultaneously at 7:28 UT. At 7:29 the second center reached its maximum and vanished at 7:31 UT, while the first became very bright at 7:32 UT (the graph shows the evolution of the intensity and area of only the first center), and reached a maximum area at 7:31 UT. After the maximum the flare gradually began to decrease both in area and in intensity. At 7:35 UT four small active centers appeared, but with lower intensities. A sharp peak was observed in the $H\alpha$ line at the center of activity and a rapid drop in intensity, with the area changing in parallel with the brightness, although the area later remained at the same level until 7:40 UT and then fell. But there was a second maximum at the center of activity from 7:40 to 7:45 UT and then for two minutes there was a rapid drop. As for the 210 MHz radio emission, no noise storm was observed from 7:20-7:27 UT, while after 7:27 UT the intensities began to increase and there were multiple bursts with different intensities $I = 36-96 \cdot 10^{-22}$ W/m²/Hz. The maximum was reached at 7:22 and 7:32 UT both in $H\alpha$ and at 1.43 m.

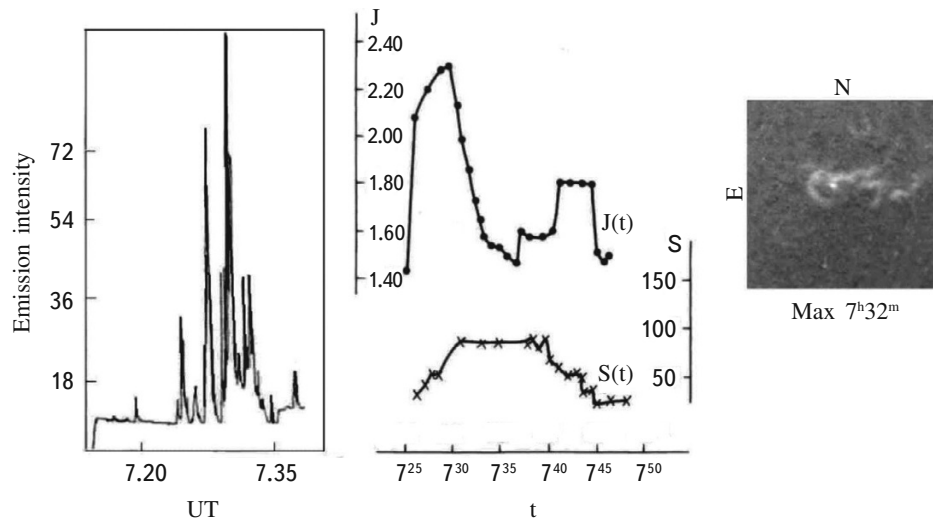


Fig. 2. Observations of flare No. 2.

Flare No. 3. July 7, 1973. (5:16-5:40 UT).

At 5:16 UT in the same flocculus, almost at the same place where flare No. 2 took place, a small intensity center lit up and another center of activity showed up in the second frame. This flare is noteworthy for its rapid rise in brightness, sharp maximum with a high intensity, and rapid fall. Both the first and the second centers reached their intensity maxima at 5:17 UT, and their maximum in area simultaneously at 5:18.5 UT (the sum $S_1(t)+S_2(t)$). The flare has gone out entirely at 5:40 UT and the area returned to its original state. The drop in the rate of fall of the intensity was a factor of three slower than for the rate of rise of the intensity. At 210 MHz a background noise storm with fairly large bursts was observed from 5:15 UT. From 5:20-5:25 UT the emission in the radio range was characterized by large bursts with an intensity of $I = 68 \cdot 10^{-22} \text{ W/m}^2/\text{Hz}$. In this case the evolution of the emission occurred almost simultaneously at the chromosphere level and in the lower corona.

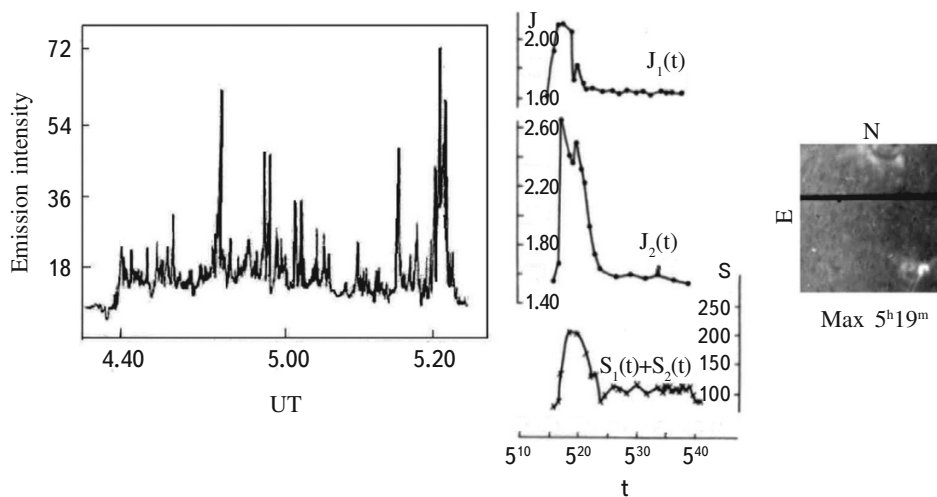


Fig. 3. Observations of flare No. 3.

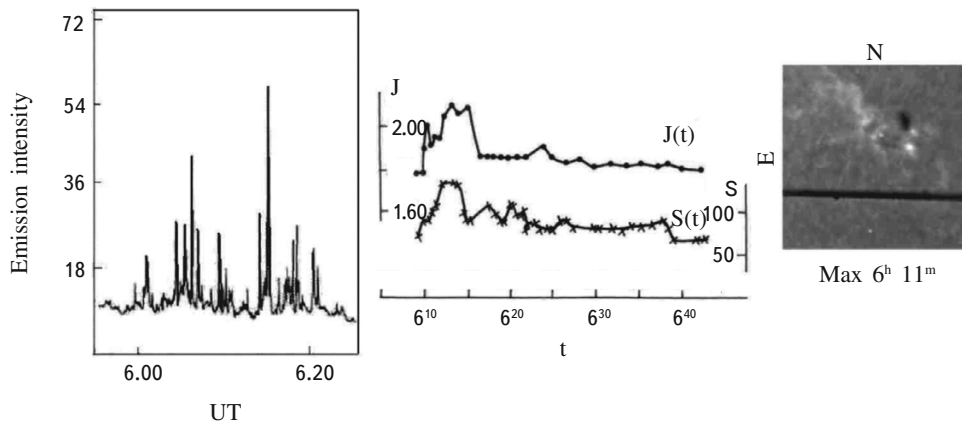


Fig. 4. Observations of flare No. 4.

Flare No. 4. July 7, 1973. (6:09-6:43 UT).

The flocculus where this flare appeared was very active right from the start. A large group of spots and two parallel filaments in the center of the flocculus were visible in the flocculus; small centers were visible at the ends of a filament and in one of these the intensity increased. At 6:13 UT the active center reached an intensity maximum, with no noticeable changes in area. Then the intensity gradually fell and after 6:30 UT until the end of the observations the center of activity stood out against the background of the flocculus.

Flare No. 5. July 9, 1973. (5:02-6:50 UT).

Several bright centers were observed in a large active flocculus at the onset of the observations. A large group of spots and a filament were observed in this flocculus; the filament began near the brightest center. This center reached an intensity maximum at 5:15 UT. After the maximum, the area of the flare increased and its intensity decreased until 5:25 UT, after which a second bright center showed up. Around 5:27 UT it reached a maximum area, and the intensity maximum occurred at 5:55 UT, after which a second bright center appeared. At 6:25 UT all the bright

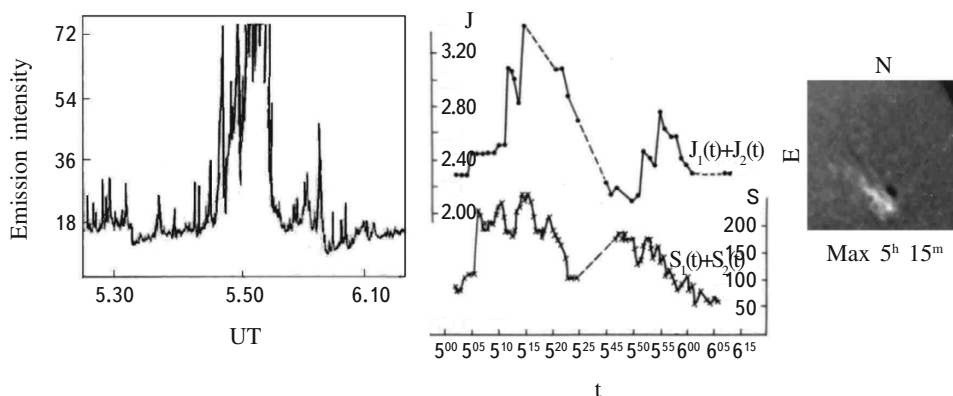


Fig. 5. Observations of flare No. 5.

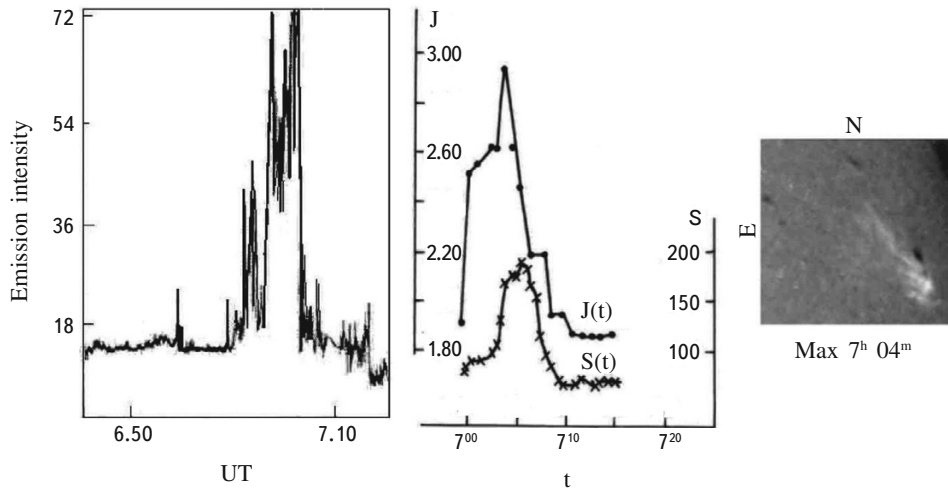


Fig. 6. Observations of flare No. 6.

centers almost disappeared and until 7:20 UT the filament in this active region hardly changed, but after 7:20 UT the entire flocculus was covered with small points of dark material.

It should be noted that this flare showed up in the same flocculus as flare No. 4. Flares No. 4 and 5 are homologous.

Flare No. 6. July 10, 1973. (7:00-7:30 UT).

At 7:00 UT an active center showed up in a large active flocculus, precisely as with flares No. 4 and 5. At 7:04 its intensity reached a maximum, and at 7:05 UT, its area. Besides the flare, an increase in the brightness of the flocculus was observed. The flare has gone out at 7:09 UT, after which the flocculus was activated anew; small active points with low activity appeared and point dark material was also observed.

Flares No. 6, 5, and 4 are homologous.

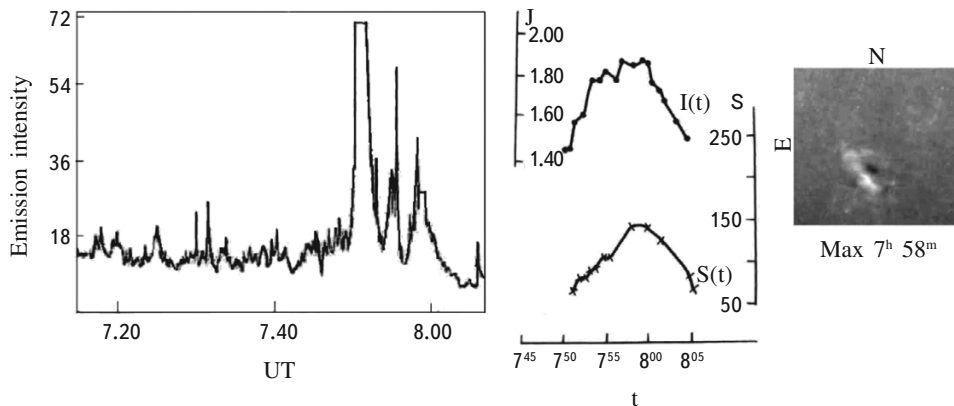


Fig. 7. Observations of flare No. 7.

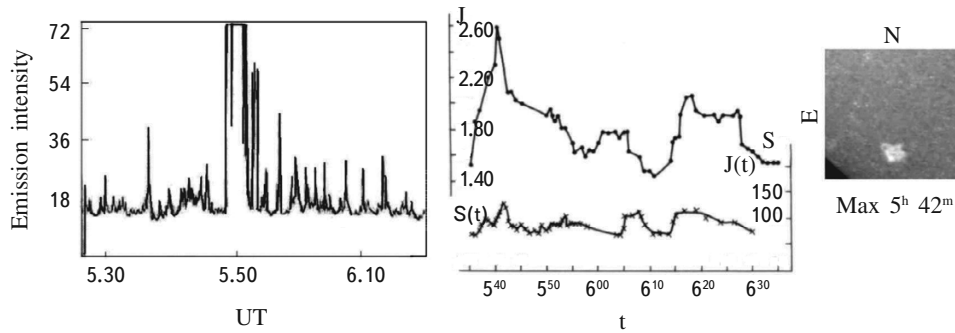


Fig. 8. Observations of flare No. 8.

Flare No. 7. August 31, 1973. (7:51-8:05 UT).

A large group of spots and even small filaments within the flocculus were observed in a large active region. At 7:51 UT an active point flared up in the spot penumbra and reached an intensity peak at 7:58 UT, but in terms of area— both the area and the intensity of the flare gradually increased. The flare has gone out at 8:05 UT. After the flare, no changes were observed in the flocculus.

Flare No. 8. September 2, 1973. (5:35-6:35 UT).

Within a small, but fairly bright flocculus a small active center appeared at 5:36 UT; its intensity increased and, in parallel with the increase in area, reached a maximum at 5:47 UT. After a few minutes the center again began to flare up and was quickly has gone out. At 6:14 UT an active center was again observed, which reached an intensity peak in parallel with the area at 6:17 UT. The flare has gone out at 6:35 UT; after this, the pattern described above was repeated two more times.

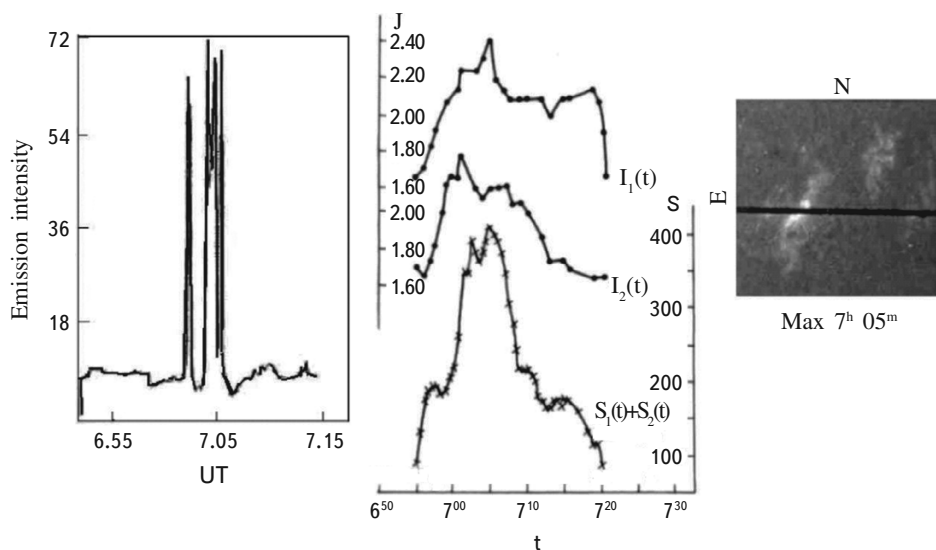


Fig. 9. Observations of flare No. 9.

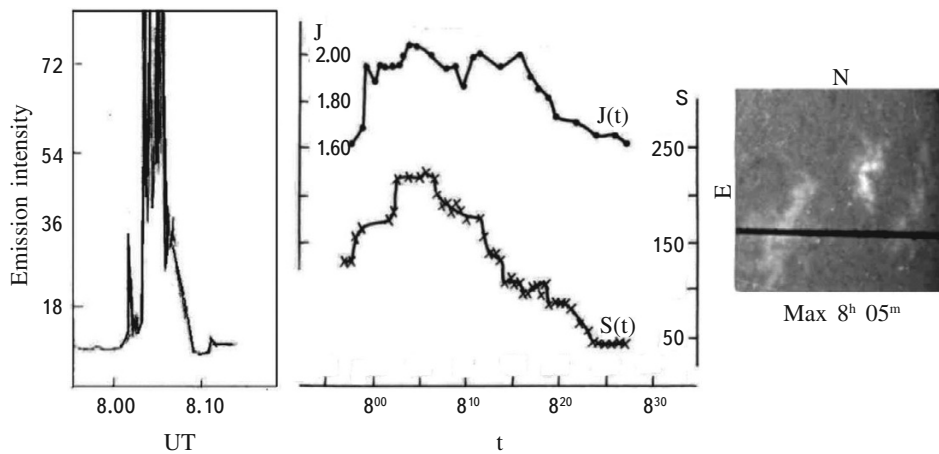


Fig. 10. Observations of flare No. 10.

Flare No. 9. September 11, 1973. (6:55-7:20 UT).

Near the western edge of the disk in a large flocculus two active regions flared up simultaneously at 6:55 UT and yet another center appeared before the maximum. In terms of intensity and area the flare reached a maximum at 7:05 UT. After the maximum, there was a noticeable enlargement in the filament which lies in the flocculus. The first two active centers has gone out earlier than the third and at approximately 7:46 UT the flare has gone out (perhaps even earlier, as clouds interfered). The filament also became smaller. The graph shows the intensity curves for the second, more intense center.

Flare No. 10. September 11, 1973. (7:58-8:27 UT).

The flare lay in a large active region. Initially two points with different intensities showed up; then they merged and formed an “S” shaped filamentary active zone. At 8:04 UT the flare reached its intensity and area maximum, after which the intensity gradually decreased and at 8:20 UT one point vanished entirely, but the second active center was seen up to the end of our observations, which ended at 8:26 UT.

Flare No. 11. September 27, 1973. (11:07-11:35 UT).

At 11:06 UT two activity centers showed up in a large flocculus. One of them was in a spot penumbra and

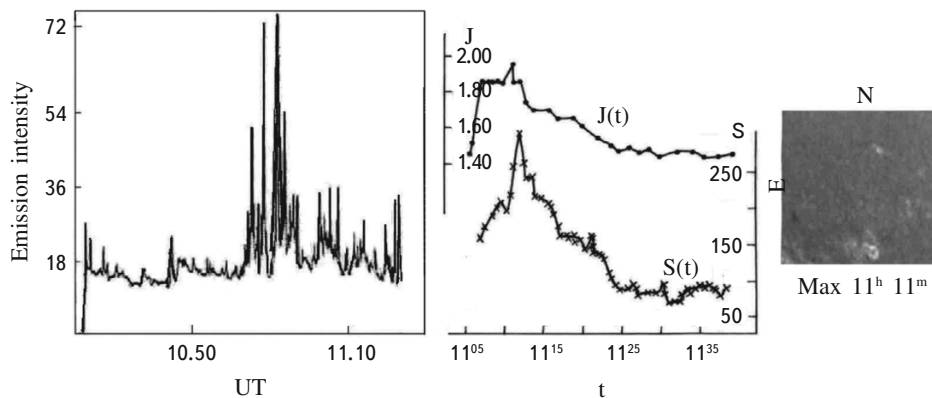


Fig. 11. Observations of flare No. 11.

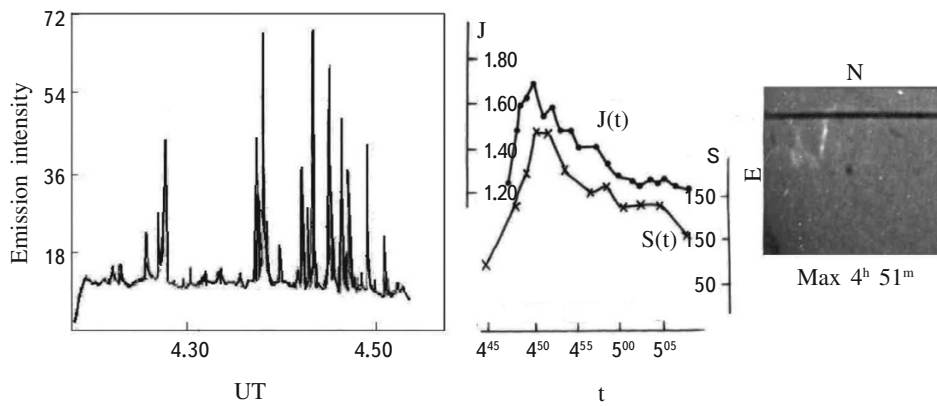


Fig. 12. Observations of flare No. 12.

after a few minutes the active centers evolved in intensity and area, simultaneously reaching a maximum at 11:11 UT. At the time of the maximum a filamentary structure appeared. The flare has gone out at 11:38 UT.

Flare No. 12. September 29, 1973. (4:47-5:06 UT).

An activity center appeared near the eastern edge near the equator in an active region at 4:46 UT. At 4:50 UT the flare reached its intensity maximum. After the maximum, the intensity of the area decreased. Besides the main center, the flare consisted of two activity centers. All of these centers merged to form a filamentary structure.

The flare has gone out at 5:06 UT. During the flare no significant changes in the flocculus were observed.

Flare No. 13. November 26, 1973. (7:04-7:13 UT).

In a large active region in a group of spots an activity center appeared at 7:04 and reached a maximum at 7:06 UT. It has gone out at 7:13 UT. Similar remarks apply to the area: it developed in parallel with the intensity. The

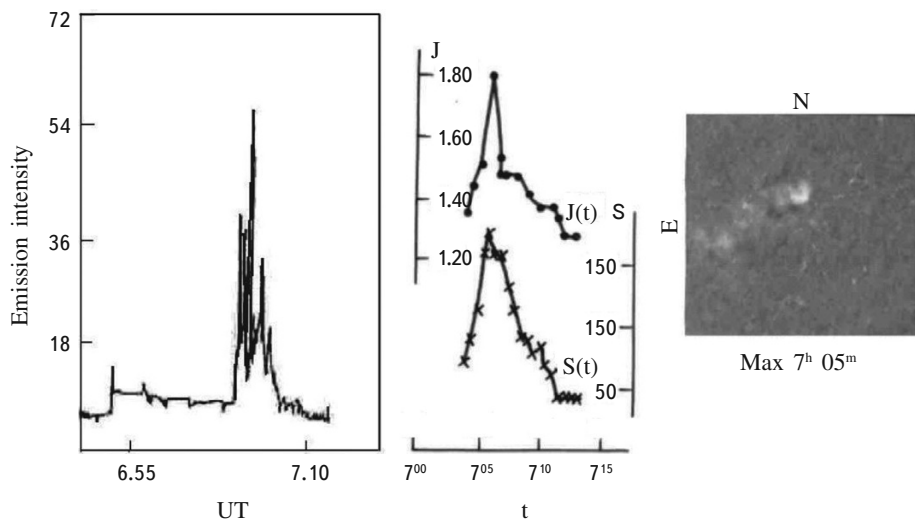


Fig. 13. Observations of flare No. 13.

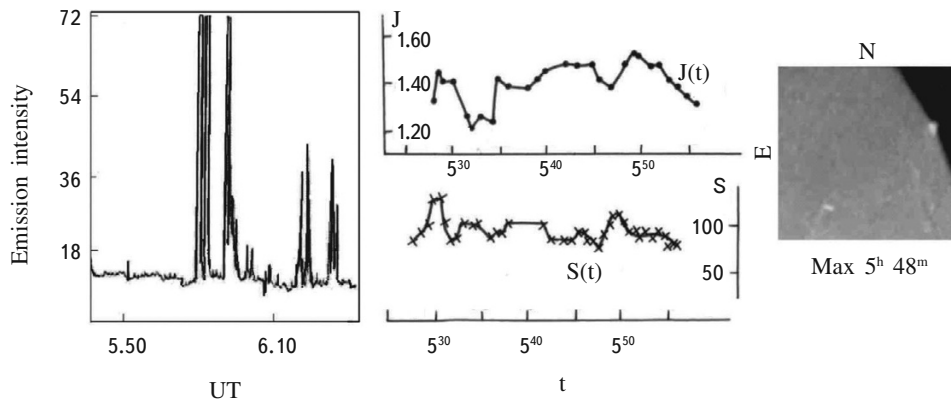


Fig. 14. Observations of flare No. 14.

filaments, which extended beyond the limits of the flocculus, propagated toward the southwest part of the solar disk. After 7:38 UT these filaments reached their greatest size and afterward one of them remained and gradually dissipated.

Flare No. 14. December 16, 1973. (5:28-11:25 UT).

In the southeast of the solar disk a single activity center lit up at approximately 5:28 UT; its intensity increased and decreased several times. From 5:40 UT a jet of matter was observed; it caused the formation of a loop protuberance and the intensity of the flare increased.

After 5:50 UT the flare decreased in intensity; a few minutes after 5:55 UT the flare could only be seen with difficulty at the edge of the disk. New ejection could be seen at approximately 6:55 UT. Later, at 7:28 UT the active center again became brighter, and at 7:04 UT the flare reached a maximum. At 8:23 UT another jet of matter from the active center appeared and in overexposed (black) frames a loop protuberance could be seen.

After 9:45 UT the intensity of the flare again increased, new maxima and new ejection appeared, and this process was repeated several times. Until the end of the observations at 11:25 UT, the flare varied continuously in area and intensity.

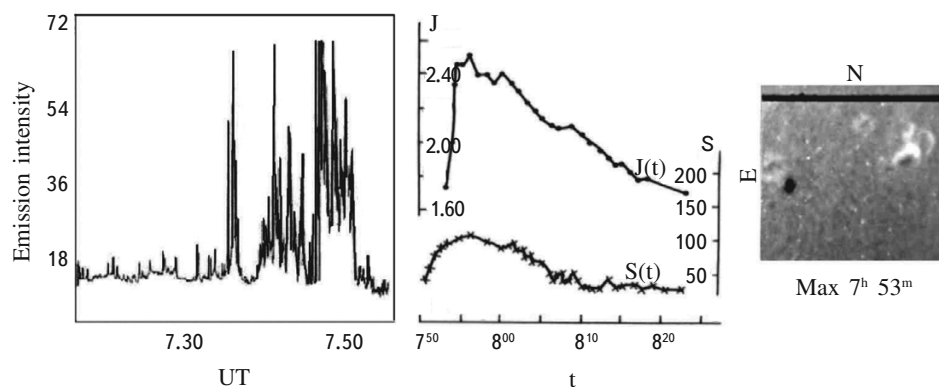


Fig. 15. Observations of flare No. 15.

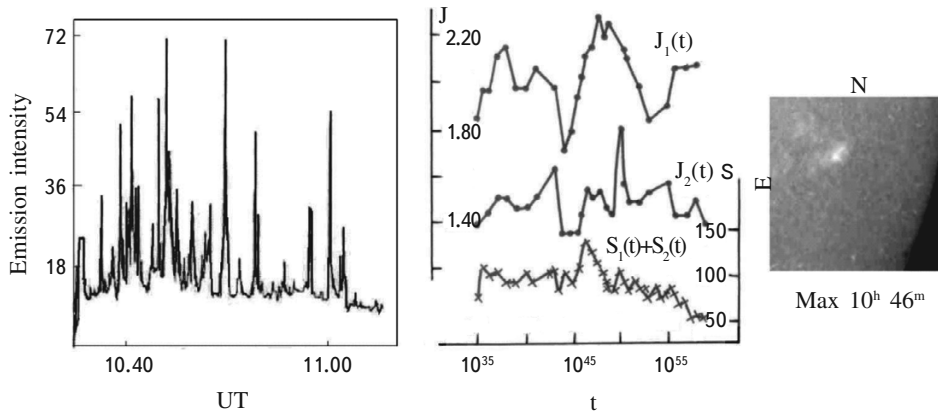


Fig. 16. Observations of flare No. 16.

Flare No. 15. December 23, 1973. (7:31-8:15 UT).

A very active center appeared at 7:51 UT in a large active region near umbra of a group of spots. Up to then several active centers (which has gone out rapidly) were noticeable in the flocculus. During the flare activation was observed in the flocculus. At 7:51 UT the intensity reached a maximum, after which, at 7:56 UT, the area increased and new, small bright centers appeared. At 8:15 the flare has gone out and the brightness of the flocculus also decreased. After roughly half an hour several active centers flared up up in the same active region, but with lower activity than the center at 7:51 UT.

Flare No. 16. December 24, 1973. (10:35-10:59 UT).

Activation was observed in the southwestern part of a rather large active flocculus. At 10:35 UT two bright centers flared up; their intensity gradually increased with the first reaching a maximum at 10:48 UT and the second, at 10:50 UT (and at 10:47 UT in terms of area). The combined area of the active centers is plotted here. At 10:59 UT the observations ended, but the first activity center had not yet has gone out.

3. Discussion and results

The major conclusions of Benz, et al. [16], are that the overall duration, peak flux, and radiated energy at radio frequencies correlate with the energy released by a flare (measured in the x-ray range). They discussed possible mechanisms for heating after the main phase of the flare and these were compared with observational data [16].

Kossobokov, et al. [17], examined 32355 class C2 and higher (C2+) flares from the GOES catalog. The amplitudes of the extreme flares increased when the average flux decreased. They calculated the average energy flux indices for an interval from 7 to 365 days [17].

Li and Fleishman [18] have calculated the incoherent radio emission in terms of two stochastic MHD heating models. Their analysis shows clearly that the radio emission from heating sites (1) is intense enough to be observed

by currently available radio instrumentation and (2) has spectra and light curves that differ distinctly in these two models. In particular, they proposed that some of the narrow-band microwave and decimeter bursts may be a consequence of stochastic heating in solar flares [18].

Based on the theory of electromagnetic radiation, equations have been derived for calculating the most intense frequencies in the spectrum of the solar radio emission. The observed frequency of the bands and the intervals between them agreed with the calculations to high accuracy. The equality of the band frequencies indicates that they are produced by interference associated with the propagation of radio waves in a plasma, rather than by a mechanism for generation of the radiation in the main source of the burst [19].

In sum, we have analyzed sixteen scale n (normal) flares in detail for the purpose of studying their motions, intensity, and development.

The development of some of the flares is accompanied by motions in the form of streams, ejection, and elongations. These motions are similar to those in the protuberances which appear after solar spots.

The development of most of the flares was accompanied mainly by a more or less uniform expansion and subsequent contraction during the extinction of flare. The intensity at the flare maximum is greater when it expands more rapidly. The maximum intensities and areas of the flares do not always coincide in time.

A detailed study of 16 chromospheric flares and the corresponding traces of 210 MHz radio emission has shown that the H α emission of some of the flares is accompanied by a rise in the emission at 210 MHz within 1/2 hour from the start or end of the flare.

By using the method of epoch superposition it is possible to determine the sequence of events during a flare. We have selected 4 times within a flare: (1) the onset of the flare in H α ; (2) the time of the maximum of the flare

TABLE 2. Time Intervals Between the Emission Peaks of Flares in H α and other Events

| Onset of flare | Precursor of noise storm | Maximum of noise storm | Onset of flare | Precursor of noise storm | Maximum of noise storm |
|----------------|--------------------------|------------------------|----------------|--------------------------|------------------------|
| -2 | -12 | 0 | -5 | -4 | -1 |
| -3 | -1 | 4 | 1 | -12 | 1 |
| -3 | 0 | 2 | -3 | -15 | -3 |
| -4 | -5 | -5 | -4 | 0 | 1 |
| -4 | -4 | 1 | -3 | -- | 2 |
| -6 | -10 | -6 | -5 | -12 | 0 |
| -7 | -5 | 9 | -3 | -6 | 0 |
| -9 | 1 | 3 | | | |

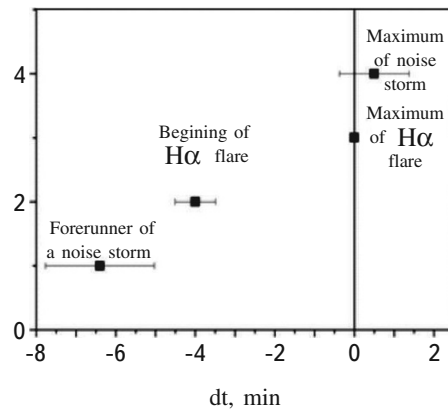


Fig. 17. Sequence of events in a flare. The vertical scale is arbitrary; the horizontal lines denote the mean square deviation from the average.

in H α ; (3) the precursor of a noise storm (a burst or group of bursts that almost always precede the main noise storm); and, (4) the maximum of the noise storm. The time of the H α flare peak was taken as the time origin. This time was subtracted from the time of the other three events for each flare to produce Table 2. On finding the average value for each column and the error in this average, we obtained the sequence of events in the optical and radio ranges during a flare (shown in Fig. 17).

In most cases (ten out of sixteen) the area of the flare reached a maximum at the same time as the intensity. In two cases, the area of the flare did not change significantly over the entire duration of the flare, and in only a few cases, the area of the flare reached a maximum just before or just after the intensity peak.

In six out of sixteen cases the maximum energy releases in the meter radio range and in the H α line were almost simultaneous, in five cases the radio peak was earlier, and in four cases the radio peak was later than in the H α line.

Observations of this type are very important for the study of fundamental problems of solar-terrestrial links. In particular, they can be used for long-term weather prediction. Recording noise storms and radio bursts of different types and comparing these with optical observations can expand our knowledge of the physical processes taking place on the sun and aid in correct interpretation of theoretical models.

REFERENCES

1. R. E. Loughhead, J. A. Roberts, and M. K. McCabe, *Austral. J. Phys.* **10**, 483 (1957).
2. R. E. Loughhead, R. A. Duncan, and J.-L. Wang, *Solar Phys.* **83**, 257 (1983).
3. E. C. Roelof, H. W. Dodson, and E. R. Hedeman, *Solar Phys.* **1957**, 339 (1983).
4. H. W. Dodson, *Proc. Inst. Radio Eng.* **46**, 149 (1958).

5. H. W. Dodson and E. R. Hedeman, *Astrophys. J.* **128**, 636 (1958).
6. H. W. Dodson and E. R. Hedeman, *Astronom. J.* **65**, 51 (1960).
7. L. D. De Feiter, A. D. Fokker, and J. Roosen, *Nature*, **184**, 805 (1959).
8. G. Swarup, P. H. Stone, and A. Maxwell, *Astrophys. J.* **131**, 725 (1960).
9. T. S. Bastian, A. O. Benz, and D. E. Gary, *Ann. Rev. Astron. Astrophys.* **36**, 131 (1998).
10. A. Vourlidas, T. S. Bastian, and M. J. Aschwanden, *Astrophys. J.* **489**, 403 (1997).
11. S. Krucker, A. O. Benz, T. S. Bastian, and L. W. Acton, *Astrophys. J.* **488**, 499 (1997).
12. K. Shibasaki, C. E. Alissandrakis, and S. Pohjolainen, *Solar Phys.* **273**, 309 (2011).
13. R. A. Greenkorn, *Solar Phys.* **280**, 205 (2012).
14. Yu. F. Yurovsky, *Bull. Crimean Astrophys. Obs.* **106**, 38 (2010).
15. Sh. Makandarashvili, *Bull. Georgian Nat. Acad. Sci.* **5**, 51 (2011).
16. A. O. Benz, H. Perret, P. Saint-Hilaire, and P. Zlobec, *Adv. Space Res.* **38**, 951 (2006).
17. V. Kossobokov, J.-L. Le Mouél, and V. Courtillot, *Solar Phys.* **276**, 383 (2012).
18. Y. Li and G. D. Fleishman, *Astrophys. J.* **701**, L52 (2009).
19. Yu. F. Yurovsky, *Bull. Crimean Astrophys. Obs.* **107**, 84 (2011).